



Study of CoFe_2O_4 @ Calixarene Core-Shell as a Novel Catalyst



Mahsa Aliakbarzadeh Roudsary¹, Karim Zare^{1*} and Majid Monajjemi²

¹Department of Chemistry, Science and Research Branch, Islamic Azad University, Tehran, Iran

²Department of Chemical engineering, Central Tehran Branch, Islamic Azad University, Tehran, Iran

*Corresponding author: Karim zare, Department of chemistry, Science and research branch, Islamic Azad university, Iran

Submission: 📅 May 14, 2018; Published: 📅 August 21, 2018

Abstract

The properties of CoFe_2O_4 @Calix [8] Core-Shell as a novel catalyst has been investigated to compare with well-known catalyst " Fe_3O_4 @Silica". It has been shown that CoFe_2O_4 magnetite particle can be used as an important catalyst inside the calix ring. In our previous papers, good results have been yielded and exhibited about the B_nN_n ring properties and CoFe_2O_4 @ B_nN_n . In present work it has been shown there is a non-covalent attraction between CoFe_2O_4 and calix [8] coated molecules. The Physical-chemistry properties such as energy densities, potential energy densities, electron densities, ELF, LOL, eta index, elasticity of electron density and ECP for CoFe_2O_4 @calix[8] shell have been calculated and simulated in related reactions for those groups-functionalized.

Keywords: CoFe_2O_4 ; Nano-particles; Electron density; calix [8]; Silica; SiO_2

Introduction

CoFe_2O_4 as the Cobalt ferrite crystallizes in a partially inverse spinel position represented as $(\text{Co}_x\text{Fe}^{3+}_{1-x})(\text{Co}^{2+}_{1-x}\text{Fe}^{3+}_{1+x})\text{O}_4$ where x based on thermal condition. It is ferri-magnetic and exhibits a relatively magnetic hysteresis which distinguishes it from the other of the spinel ferrites. Magnetic measurements on nano-particles of cobalt ferrite dispersed in various solvents of organic compounds and nano-crystalline powders prepared by hydroxide precipitation have been investigated earlier. In magnetic fluids, it has been seen that for particles above three nano-meters the saturation magnetization remains constant at about 30 emu g^{-1} that is extensively less than the bulk values [1-5].

Magnetic Nan-Oparticles (MNPs) have shown exceptional potential for several biological and clinical applications. However, MNPs might be coated by the biocompatible shells for such applications. The aim of this study is to understand if and how the surface charges and coatings can affect the magnetic and electronic properties of Cobalt ferrite crystallizes. The role of the surfaces on the magnetic moments of a magnetic nano particle such as CoFe_2O_4 is an important issue, and various effects can contribute for making it deviate from the bulk value, including the charges, the nature of the coating, also the synthetic technique. The electronic properties and ionic distribution of CoFe_2O_4 NPs were probed by X-ray absorption spectroscopy, X-ray-magnetic-circular-dichroism and X-ray-photoemission-spectroscopy-techniques known as the abbreviation XAC, XMCD and XPS respectively. Magnetite-

particles are also of interests in medicinal and industries application such as Magnetic-Resonance-Imaging (MRI) or organic catalyst and nano-material synthesis [4-8].

The overall magnetic behavior and the hyper-thermic properties were evaluated by magnetometers and molecular modelling measurements, respectively. The results show that all of the investigated CoFe_2O_4 NPs have high magnetic anisotropy energy, and the surface charges and coating do not influence appreciably their electronic and magnetic properties. In addition, the citrate shell improves the stability of the NPs in aqueous environment, making CoFe_2O_4 NPs suitable for biomedical applications. Magnetic nano-particle exhibits several unique properties such as super-paramagnetism compared to bulk material and particularly, are used in the field of biology and medicines. Magnetic nano-particle has attracted a great deal of research interests due to their distinctive properties and special application recently [5-9]. CoFe_2O_4 is a well-known hard magnetic material with very high cubic magneto-crystalline anisotropy, high coercivity and moderate saturation magnetization. These properties make it a promising material for high-density magnetic recording. The most applications require at least a magnetic-particle for dispersing in the non-magnetic matrixes. This matrix plays an important role for providing the meaning of particle dispersion for determining a physical property of a composite.

Recently, in the sol-gel synthesis of CoFe_2O_4 particles, the gel is built-up via physical and chemical bonds between the chemical species. It has been introduced a different sol-gel route via polyacrylamide gel route for preparing CoFe_2O_4 nano-particle. Due to lack of controls over the specific transformation of a nano-particle, obviously super-paramagnetic particle has not been prepared from magnetite, i.e. Magnetite-nano-particle which generally loses their permanent magnetic properties in the lack of the external magnetic field [6-10]. The complex of metal- $\text{CoFe}_2\text{O}_4@ \text{SiO}_2\text{-NH}_2$ nano-particles could be recovered easily from aqueous through magnetic separation and reproduced readily by acid treatment. By this work it has been exhibited the amino-functionalized $\text{CoFe}_2\text{O}_4@ \text{calix}$ [8] magnetic nano-particles compare to $\text{CoFe}_2\text{O}_4@ \text{SiO}_2$ is much more effective as recyclable adsorbent for the removal of heavy and alkali/earth metal ions in water and wastewater treatments. Silica shells chemically is stable and can be rapidly functionalized in the bio-conjugation purposes, in other words is biocompatible therefore $\text{CoFe}_2\text{O}_4@ \text{SiO}_2$ as a silica coated magnetite composite nano-particles have been synthesized by several groups. Catalysts have a very sensitive treatment in technology and modern sciences as they increase reaction yield via reducing the temperature in synthesis of the chemical product. There are two basic types of catalysis, heterogeneous, where the reaction accomplishes on the surfaces and the catalysts are in the solid phase. Homogeneous, where the catalyst is in one phase as reactant. The other important items of these matrixes are to act as a protection for magnetic nano-particles against oxidation or corrosion especially in the metallic nano-particles. Among oxide matrixes such as alumina, silica, zeolites, titanic oxides, carbon-based, the silica can be a general suitable material for the matrixes because of inertness of the magnetic fields, its non-toxicity and easiness for forming cross-linked networks structure [10-17]. The bridge between heterogeneous and homogeneous catalysts can be attained through the CoFe_2O_4 nanoparticle [17-25]. CoFe_2O_4 exclusively is useful and important as the magnetic nano-particle which exhibit strong magnetic-moment and are seldom sustained outside of an external magnetic field. These kinds of nano-particle might be consist of several materials such as nickel, cobalt, iron oxides, and ferrites and also alloys such as platinum/iron. CoFe_2O_4 MNPs of silica shells catalytic materials have the benefit for increasing surface area which causes for any increased reaction rate. Moreover, nano-particle might permit additional catalytic functionality because of their unique properties. Several catalysis of magnetic nano-structure has been investigated up to now, such as preparation of nano-composite materials consist of magnetic-(core) nano-particle which has been coated by various shells of other catalytically active nano-material [20-30].

Other type of catalysts that are interest for organic compounds involves the using of organic molecules which are enabling for preservation of the materials in the end of any reactions for reusing [25-35]. In this work we have investigated the catalysis's properties of CoFe_2O_4 nano-particles @calix [8] instead of SiO_2 for comparing in chemical syntheses [36-47]. Recently extensive theoretical and experimental studies have been accomplished on boron-nitride-fullerenes for understanding their relative stabilities also

size dependence of important physical properties. In our previous works [48-61], it has been exhibited the system stabilities, NMR data, electronic properties, and chemical phenomenon.

Background & Methodology

Magnetic particles are suitable for aqueous transition and heavy metals due to their unique advantages of quick separation and their high surface area under external magnetic fields [62-65]. The surface modification, adsorption affinity, including covalent binding and physical coating, has often been explored for enabling specific complexation for further facilitates [66-70]. Recently it has been exhibited which the amino-functionalized molecules demonstrated outstanding abilities for removing a wide variety of transition heavy metal ions [71-76]. Although $\text{CoFe}_2\text{O}_4@ \text{SiO}_2$ has recently been investigated for potential biomedical applications [77-81], there is no work about the $\text{CoFe}_2\text{O}_4@ \text{calix}$ [8].

In this study with the theoretical approaches magnetic an adsorbent has been developed via covalently grafting amino groups over the surfaces of $\text{CoFe}_2\text{O}_4@ \text{calix}$ [8] nano-particles. Part of the systems including $\text{CoFe}_2\text{O}_4@ \text{calix}$ [8] nano-particles has been simulated with QM/MM methods and the investigation carried out by the Monte Carlo calculations. In this study, various force fields are done via "Amber" and OPLS for comparing the calculated energy of the $\text{CoFe}_2\text{O}_4@ \text{calix}$ [8] nano-particles. Furthermore, a Hyper-Chem professional release-7.01 program is used for any further calculations. The density functional method is used for the high level while the semi-empirical (pm_6) with pseudo-Lan₂ and Pm_3MM for both of them respectively. Some accurate studies have indicated that inaccuracy of the low range exchange energies goes to the large systematic errors for the prediction of molecular properties.

Geometries optimization and electronic calculations have been accomplished using the m06 functional of DFT. These approaches are based on solution of the Kohn & Sham [82] in the plane-waves sets with projector-augmented-pseudo-potentials. The Perdew & Burke [83] exchange-correlation and generalized-gradient-approximation GGA are also used for non-bonding calculation.

The charge transferring and electrostatics potentials derived charges were also estimated using the Merz & Kollman [84]; [85,86]. The charges calculation methods based on MESP or molecular-electrostatics-potentials fitting are not well suited for the larger systems whereas several of the inner-most points are located far away from the centers at which the MESP are computed. In that position, variation of the inner-most atomic charges would not be towards the changing of the MESP outside of the molecules [87,88]. The interaction energies or adsorbents energies between metals and $\text{CoFe}_2\text{O}_4@ \text{calix}$ [8] catalyst were done according to the equation as follows:

$$\Delta E_s (eV) = \left\{ E_c \left(\sum_{i=1}^n (\text{metal-CoFe}_2\text{O}_4\text{-Calix}[8])_i + \sum_{j=1}^m (\text{CoFe}_2\text{O}_4)_j + \sum_{v=1}^q \text{calix}[8]_v \right) + \sum_{k=1}^p \text{metal-ion}_k \right\} + E_{BSSE} \quad (1)$$

That ΔE_s is the adsorbents energies. The electron-localization-function or ELF, localized-orbital-locator or LOL [89-91], electron

density of the Gradient-norm & Laplacian, values of orbitals wave-functions, electron spin densities, electrostatic-potentials from nuclear-atomic-charges, the exchange-correlation density, as well as total electrostatic potentials (ESP), correlation-holes and correlation-factors, and the average local ionization energies using the Multi-functional-Wave-function analyzer have also been calculated in this study [89-91].

Density Electron Approach for Interaction between Mnps and Calix [8]

The kinetic energies densities are not defined individually, since the expected values of the operators:

$$\langle \varphi | -\left(\frac{1}{2}\right) \nabla^2 | \varphi \rangle \quad (2)$$

Can be estimated by integrating kinetic energy densities from those alternative definitions. One of the usual used definitions is as follows:

$$k(r) = -\frac{1}{2} \sum_i \eta_i \varphi_i^*(r) \nabla^2 \varphi_i(r) \quad (3),$$

The local kinetic energies given below guarantee [89-91] hence the physical data are more commonly used. The Lagrangian of kinetic energies densities, $G(r)$ are also known as positive definite kinetic energy densities.

$$G(r) = \frac{1}{2} \sum_i \eta_i |\nabla(\varphi_i)|^2 = \frac{1}{2} \sum_i \eta_i \left\{ \left(\frac{\partial \varphi_i(r)}{\partial(x)}\right)^2 + \left(\frac{\partial \varphi_i(r)}{\partial(y)}\right)^2 + \left(\frac{\partial \varphi_i(r)}{\partial(z)}\right)^2 \right\} \quad (4)$$

$K(r)$ and $G(r)$ are directly related by Laplacian of electron density $\frac{1}{4} \nabla^2 \rho(r) = G(r) - K(r)$. The electrostatic potential from nuclear/atomic charges can be calculated via: $V_{\text{muc}}(r) = \sum_A \frac{Z_A}{|r-R_A|}$ where R_A and Z_A denote position vector and nuclear charge of atom A, respectively, spherically averaged like-spin conditional pair probability have correlation with the Fermi hole and it has been suggested which the electron localization function (ELF).

$$ELF(r) = \frac{1}{1 + [D(r)/D_{0(r)}]^2} \quad (5)$$

$$\text{Where } D(r) = \frac{1}{2} \sum_i \eta_i |\nabla \varphi_i|^2 - \frac{1}{8} \left[\frac{|\nabla \rho_\alpha|^2}{\rho_\alpha(r)} + \frac{|\nabla \rho_\beta|^2}{\beta(r)} \right]$$

and

$$D_{0(r)} = \frac{3}{10} (6\pi^2)^{\frac{2}{3}} [\rho_\alpha(r)^{\frac{5}{3}} + \rho_\beta(r)^{\frac{5}{3}}] \quad (6)$$

for close-shell system, since

$$\rho_\alpha(r) = \rho_\beta(r) = \frac{1}{2} \rho$$

and D_0 terms can be simplified as

$$D(r) = \frac{1}{2} \sum_i \eta_i |\nabla \varphi_i|^2 - \frac{1}{8} \left[\frac{|\nabla \rho|^2}{\rho(r)} \right], D_{0(r)} = \frac{3}{10} (3\pi^2)^{\frac{2}{3}} \rho(r)^{\frac{5}{3}}$$

In which the kinetic energies terms in $D(r)$ is replaced by Kirzhnits types second-order gradients expansion, which are

$$\frac{1}{2} \sum_i \eta_i |\nabla \varphi_i|^2 \approx D_{0(r)} + \frac{1}{72} \frac{|\nabla \rho|^2}{\rho(r) + \frac{1}{6} \nabla^2 \rho(r)} \quad (7)$$

So that ELF is totally independent from the wave-function, and then can be used for analyzing electron densities from X-ray diffraction data. Localized orbital locator or LOL is another item for locating high localization regions likewise ELF, which explained by Lu T [91].

$$LOL(r) = \frac{\tau(r)}{1 + \tau(r)},$$

Where

$$\tau(r) = \frac{D_{0(r)}}{\frac{1}{2} \sum_i \eta_i |\nabla \varphi_i|^2} \quad (8)$$

for spin-polarized system and close-shell system are defined in the same way as in ELF. LOL have similar approaches compared to ELF. Notice that evaluating ESP is much more time-consuming than evaluating other functions. The ESP evaluated under default value is accurate enough in general cases. Reduced density gradient (RDG) RDG are a pair of very important functions for revealing weak interaction region for detail. RDG is defined as

$$RDG(r) = \frac{1}{2(3\pi^2)^{\frac{1}{3}}} \frac{|\nabla \rho(r)|}{\rho(r)^{\frac{4}{3}}} \quad (9).$$

Fortunately, it is found that weak interaction analysis under pro-molecular density is still reasonable. Pro-molecular density is simply constructed by superposing electron densities of free-state atoms and hence can be evaluated extremely rapidly. $\rho^{\text{pro}}(r) = \sum_A \rho_A^{\text{free,fit}}(r-R_A)$. Where $\rho_A^{\text{free,fit}}$ is a pre-fitted spherically averaged electrons density of atom A.

Result and Discussion

Table 1: (a) All Electron Densities of non-bonded interactions for CoFe_2O_4 @Silica shell, (b) CoFe_2O_4 @calix[8] shell and (c) CoFe_2O_4 (isolate).

Atoms of CoFe_2O_4	Density of All Electron (10^{-3})			Density of Alpha (10^{-3})			Density of Beta (10^{-3})			Spin Density		
	(a)	(b)	(c)	(a)	(b)	(c)	(a)	(b)	(c)	(a)	(b)	(c)
Co(1)	0.28	0.32	0.12	0.14	0.16	0.06	0.14	0.16	0.06	0.0	0.0	0.1
Fe(2)	0.28	0.3	0.1	0.14	0.15	0.05	0.14	0.15	0.05	0.0	0.0	0.1
Fe(3)	0.16	0.28	0.12	0.08	0.14	0.06	0.08	0.14	0.06	0.0	0.0	0.1
O(1)	0.3	0.24	0.14	0.15	0.12	0.07	0.15	0.12	0.07	0.0	0.0	0.0

O(2)	0.18	0.32	0.12	0.09	0.16	0.06	0.09	0.16	0.06	0.0	0.0	0.0
O(3)	0.3	0.22	0.16	0.15	0.11	0.08	0.15	0.11	0.08	0.0	0.0	0.0
O(4)	0.14	0.2	0.18	0.07	0.1	0.09	0.07	0.1	0.09	0.0	0.0	0.0

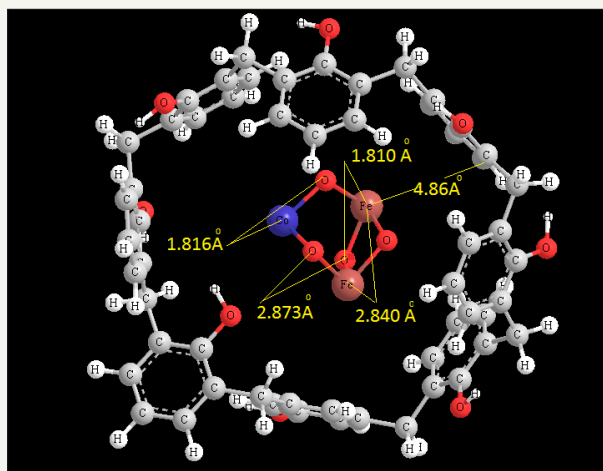


Figure 1: The non-bonded interaction between CoFe_2O_4 and Calix [8] shell.

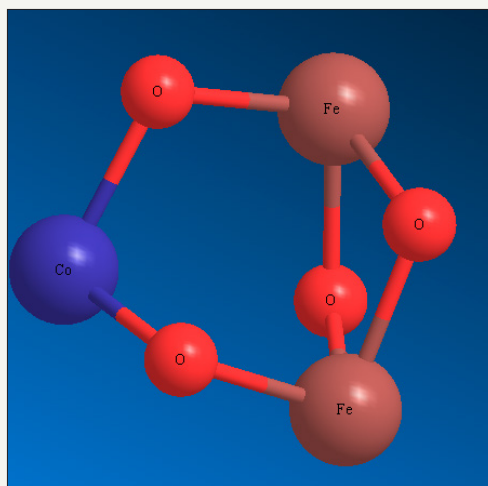


Figure 2: The optimized of CoFe_2O_4 .

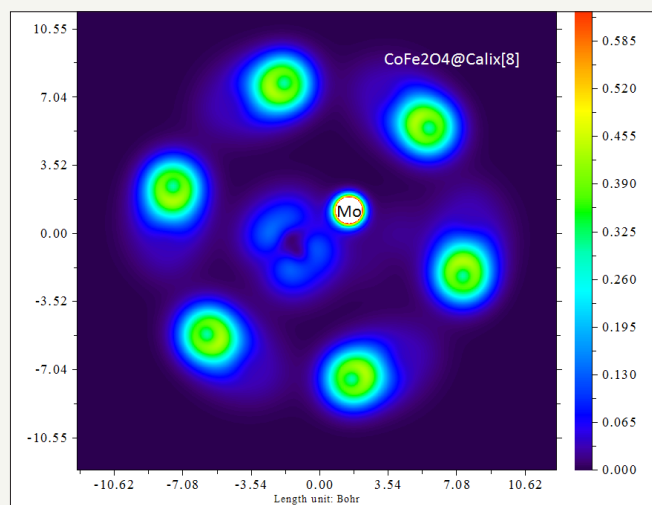


Figure 3: Color field map of electro density including molybdenum & CoFe_2O_4 inside of Calix [8].

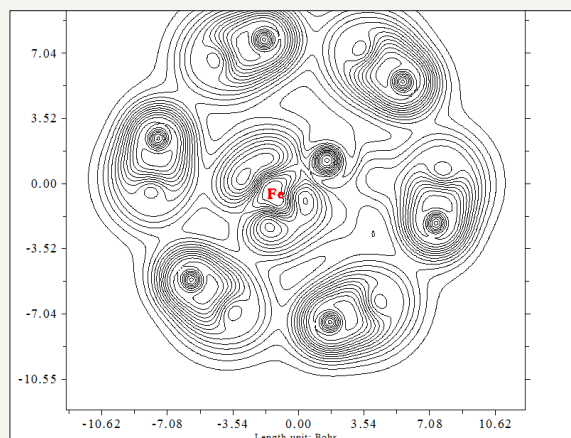


Figure 4: Contour line map of CoFe_2O_4 -Calix [8] for LOL.

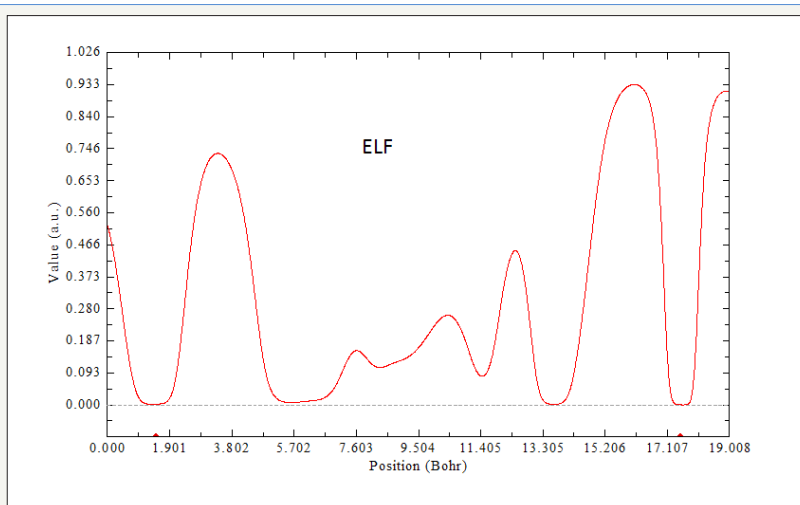


Figure 5: ELF versus Position for CoFe_2O_4 @calix[8] & Mo.

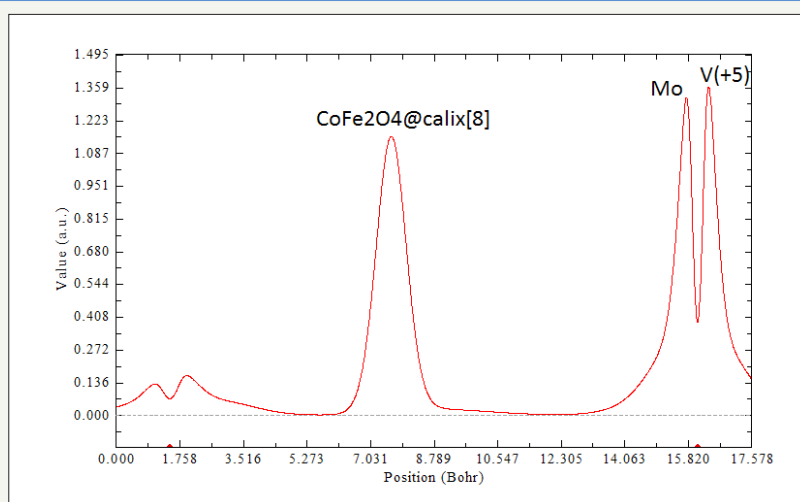


Figure 6: Pick Position for CoFe_2O_4 @calix[8] Mo & V (+5).

This work basically focuses on the magnetic properties of CoFe_2O_4 in the non-bonded systems with calix[8] surfaces including " CoFe_2O_4 @calix [8]". The CoFe_2O_4 @calix[8] nano-adsorbent shown high adsorption affinities for aqueous metal especially for

cation of vanadium and molybdenum and the amino- CoFe_2O_4 @ SiO_2 exhibited high adsorbent for vanadium and molybdenum ions, resulting from complexation of the metal ion with the surface amino groups. The metalloaded CoFe_2O_4 @calix[8] nano-particles could

be recovered easily from aqueous solution by magnetic separation. The data have shown in Figure 1-7 and Table 1. As it is indicated in Table 1, LOL is low and constant for Both CoFe_2O_4 @silica, CoFe_2O_4 @calix[8] and CoFe_2O_4 @calix [8]. ELF has a similar expression as LOL. The non-bonded interactions are shown in Figure 1-7. The electrical properties can be obtained from changes in the non-

bonded interactions. Potential energy densities, ELF, LOL, electron densities, energy densities, eta index and ECP are shown Table 1. The results of ELF and LOL indicate that the surfaces of silica and calix [8] are suitable to attach in aromatic and organic compounds in any scale from nano to micro or medium.

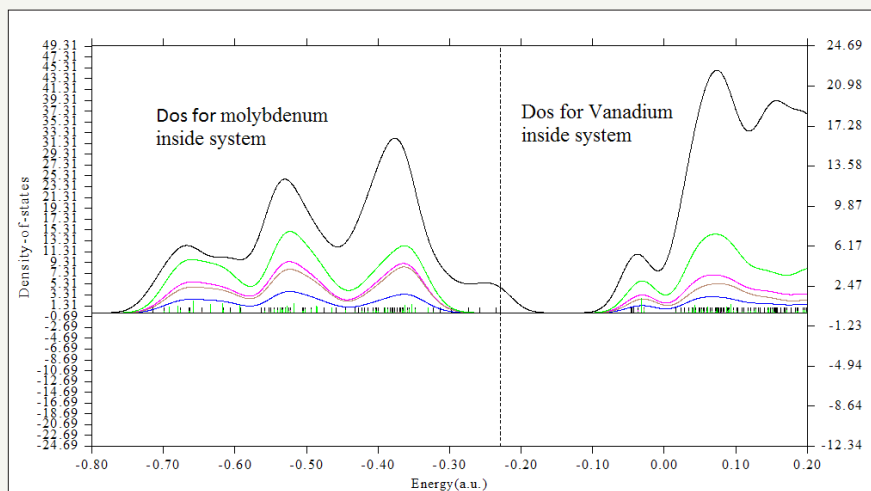


Figure 7: Density of state for energy absorption of Molybdenum and Vanadium in CoFe_2O_4 @Calix[8].

The interaction energy between two sides of CoFe_2O_4 -silica and CoFe_2O_4 -calix [8] are also calculated Table 1. This problem will be removed by replacing the calix[8] instead of SiO_2 as a shell of CoFe_2O_4 . In addition, functional groups on the coating layer chemically adhering to the MNPs are also available to acid treatment. In contrast of SiO_2 rings which is stable under acidic conditions the calix [8] rings are independent from acidic situations and hence for calix[8] comparing to SiO_2 , the function is not needed as an ideal shell composite to protect the inner magnetite core. Although CoFe_2O_4 @ SiO_2 or Silica-coated core-shell magnetite nanoparticles have recently been investigated for potential biomedical applications, by this work we exhibit the calix [8] is much useful for removing the earth/alkali metal from the aqueous solution Table 1. Relative adsorption energies of four transition metal ions such as vanadium and molybdenum on CoFe_2O_4 @calix[8] have been investigated.

Conclusion

We think that calix[8] capabilities of magnetic substrates should be explored in the near future. Another interesting development is using the calix[8] on magnetic-nano-particle enables effective removal of transition metals such as vanadium and molybdenum metals based on catalysts forms important pharmaceutical products in the drug nanotechnology. Our calculations indicate that the calix[8] is suitable surfaces for CoFe_2O_4 such silica surfaces for removal metal ions such as vanadium cations and molybdenum.

References

- Massart R (1981) Preparation of aqueous magnetic liquids in alkaline and acidic media IEEE transactions on magnetics 17(2): 1247-1248.
- Valter S, Richard TO, Rao KV (2010) Real-time monitoring of the evolution of magnetism during precipitation of superparamagnetic nanoparticles for bioscience applications. J Mater Chem 20: 4168-4175.
- Shi M, Zuo RZ, Xu YD, Jiang YZ, Yu GY, et al. (2012) Preparation and characterization of CoFe_2O_4 powders and films via the sol-gel method. J Alloy Compd 512: 165-170.
- Cui HT, Jia YY, Ren WZ, Wang WH (2010) Facile and ultra-large-scale synthesis of nearly monodispersed CoFe_2O_4 nanoparticles by a low temperature sol-gel route. Journal of Sol-Gel Science and Technology 55(1): 36-40.
- Burianova S, Vejpravova JP, Holec P, Plocek J, Niznansky D (2011) Surface spin effects in La-doped CoFe_2O_4 nanoparticles prepared by microemulsion route. J Appl Phys 110: 073902.
- Haneda K, Morrish AH (1998) J Appl Phys 63(8): 42-58.
- Moumen N, Veillet P, Pileni MP (1995) Controlled preparation of nanosize cobalt ferrite magnetic particles. Journal of Magnetism and Magnetic Materials 49(1-2): 67-71.
- Blaskov V, Petkov V, Rusanov V, Martinez LM, Martinez B, et al. (1996) Magnetic properties of nanophase CoFe_2O_4 particles. Journal of Magnetism and Magnetic Materials 162(2-3): 331-337.
- Pillai V, Shah DO (1996) Synthesis of high-coercivity cobalt ferrite particles using water-in-oil micro-emulsions. Journal of Magnetism and Magnetic Materials 163(1-2): 243-248.
- Davis KJ, Well S, Upadhyay SV, Charles SW, OGrady KM, et al. (1995) The observation of multi-axial anisotropy in ultrafine cobalt ferrite particles used in magnetic fluids. Journal of Magnetism and Magnetic Materials 149(1-2): 14-18.
- Ming M, Yu Z, Zhir G, Ning GU (2013) Facile synthesis of ultrathin magnetic iron oxide nanoplates by Schikorr reaction. Nanoscale Research Letters 8(1): 16.
- Zhu ZG, Li XY, Zhao QD, Shi Y, Li H, et al. (2011) Surface photovoltage properties and photocatalytic activities of nanocrystalline CoFe_2O_4 particles with porous superstructure fabricated by a modified chemical coprecipitation method. Journal of Nanoparticle Research 13(5): 2147-2155.
- Zhang Y, Liu Y, Yang Z, Xiong R, Shi J (2011) Synthesis of CoFe_2O_4 nanoparticles with tunable magnetism by the modified hydrothermal method. Journal of Nanoparticle Research 13: 4557.

14. Peng JH, Hojamberdiev M, Xu YH, Cao BW, Wang J, et al. (2011) Hydrothermal synthesis and magnetic properties of gadolinium-doped CoFe_2O_4 nanoparticles. *Journal of Magnetism and Magnetic Materials* 323: 133-137.
15. Yanase A, Siratori K (1984) Band structure in the high temperature phase of Fe_3O_4 . *J Phys Soc Jpn* 53: 312-317.
16. Peñicaud M, Siberchicot B, Sommers CB, Kubler J (1992) Calculated electronic band structure and magnetic moments of ferrites. *Journal of Magnetism and Magnetic Materials* 103(1-2): 212-220.
17. Babes L, Denizot B, Tanguy G, Le Jeune JJ, Jallet P (1999) Synthesis of iron oxide nanoparticles used as MRI contrast agents: A parametric study. *Journal of Colloid and Interface Science* 212(2): 474-482.
18. Berry C, Curtis ASG (2003) Functionalisation of magnetic nanoparticles for applications in biomedicine. *Journal of Physics D: Applied Physics* 36(13): R198-R206.
19. Ruuge EK, Rusetski AN (1993) Magnetic fluids as drug carriers: Targeted transport of drugs by a magnetic field. *Journal of Magnetism and Magnetic Materials* 122(1-3): 335-339.
20. Pope NM, Alsop RC, Chang YA, Smith AK (1994) *J Biomed Mater Res* 2: 449-457.
21. Tago T, Hatsuta T, Miyajima K, Kishida M, Tashiro S, et al. (2002) Novel synthesis of silica-coated ferrite nanoparticles prepared using water-in-oil microemulsion. *Journal of the American Ceramic Society* 85(9): 2188-2194.
22. Lei Z, Li YL, Wei XY (2008) A facile two-step modifying process for preparation of poly(SSNa)-grafted $\text{Fe}_3\text{O}_4/\text{SiO}_2$ particles. *Journal of Solid State Chemistry* 181(3): 480-486.
23. Huang C, Bin H (2008) Silica-coated magnetic nanoparticles modified with γ -mercaptopropyltrimethoxysilane for fast and selective solid phase extraction of trace amounts of Cd, Cu, Hg, and Pb in environmental and biological samples prior to their determination by inductively coupled plasma mass spectrometry. *Spectrochim Acta Part B: Atomic Spectroscopy* 63(3): 437-444.
24. Philipse AP (2011) Heterogeneous catalysis: On bathroom mirrors and boiling stones. *J Chem Educ* 88(1): 59-62.
25. Sheldon RA, Downing RS (1999) Heterogeneous catalytic transformations for environmentally friendly production. *Applied Catalysis A: General* 189(2): 163-183.
26. Hamilton DJ (2003) Homogeneous catalysis-New approaches to catalyst separation, recovery, and recycling. *Science* 299(5613): 1702-1706.
27. Cornils B, Herrmann WA (2003) Concepts in homogeneous catalysis: the industrial view. *Journal of Catalysis* 216(1-2): 23-31.
28. Johnson BG (2003) Nanoparticles in catalysis. *Topics in Catalysis* 24(1-4): 147-159.
29. Laurent S, Forge D, Port M, Roch A, Robic C, et al. (2008) Magnetic iron oxide nanoparticles: synthesis, stabilization, vectorization, physicochemical characterizations, and biological applications. *Chem Rev* 108(6): 2064-2110.
30. Kodama RH (1999) Magnetic nano-particles. *Journal of Magnetism and Magnetic Materials* 200(1-3): 359-372.
31. Chang LL, Erathodiyil N, Ying JY (2012) Nanostructured catalysts for organic transformations. *Acc Chem Res* 46(8): 1825-1837.
32. Fujishima A, Zhang X, Tryk DA (2008) TiO_2 photocatalysis and related surface phenomena. *Surface Science Reports* 63(12): 515-582.
33. Wang X, Gaiano SM, Bridges T, Montell D (2008) *ProtocExch* 28.
34. Wei S, Wang Q, Zhu J, Sun, L, Lin, et al. (2011) Multifunctional composite core-shell nanoparticles. *Nanoscale* 3(11): 4474-4502.
35. Yoon TJ, Lee W, Oh YS, Lee JK (2003) Magnetic nanoparticles as a catalyst vehicle for simple and easy recycling. *New Journal Chemistry* 27(2): 227-229.
36. Yu Zh, Hu ML, Zhang CX, Sun LZ, Zhong JJ (2011) Tunneling magneto resistance of bilayer hexagonal boron nitride and its linear response to external uniaxial strain. *J Phys Chem C* 115(16): 8260-8264.
37. Seifert G, Flower PW, Mitchell D, Porezag D, Frauenheim T (1997) Boron-nitrogen analogues of the fullerenes: electronic and structural properties. *Chemical Physics Letters* 268(5-6): 352-358.
38. Alexandre SS, Chacham H, Nunes RW (1999) Stability, geometry, and electronic structure of the boron nitride $\text{B}_{36}\text{N}_{36}$ fullerene. *Appl Phys Lett* 75: 61.
39. Locke IW, Darwish AD, Kroto HW, Prassides K, Taylor R, et al. (1994) Phosphorus/buckminsterfullerene intercalation compounds, $\text{C}_{60}(\text{P}_4)_2$. *Chemical Physics Letters* 225(1-3): 186-190.
40. Behrman EC, Foehrweiser RK, Myers JR, French BR, Zandler ME (1994) Possibility of stable spheroid molecules of ZnO. *Phys Rev A* 49: R1543.
41. Kaxiras E, Jackson K, Pederson MR (1994) Theoretical study of passivated small fullerenes C_{24}X_4 (XN, PAs) and their isoelectronic equivalents $(\text{BN})_{12}\text{X}_4$. *Chemical Physics Letters* 225(4-6): 448-453.
42. Zhao JX, Ding YH (2008) Theoretical study of Ni adsorption on single-walled boron nitride nano-tubes with intrinsic defects. *J Phys Chem C* 112(15): 5778-5783.
43. Bagheri S, Moosavi MS, Moradiyeh N, Zakeri M, Attarikhsharaghi N, et al. (2015) *Molecules* 20: 21636-21657.
44. Strout DL (2004) Fullerene-like cages versus alternant cages: isomer stability of $\text{B}_{13}\text{N}_{13}$, $\text{B}_{14}\text{N}_{14}$, and $\text{B}_{16}\text{N}_{16}$. *Chemical Physics Letters* 383(1-2): 95-98.
45. Zope RR, Dunlap BI (2004) Are hemispherical caps of boron-nitride nanotubes possible? *Chemical Physics Letters* 386(4-6): 403-407.
46. Zope RR, Baruah T, Pederson MR, Dunlap BI (2004) Electronic structure, vibrational stability, infrared, and Raman spectra of $\text{B}_{24}\text{N}_{24}$ cages. *Chemical Physics Letters* 393(4-6): 300-304.
47. Zheng JW, Zheng LP, Wu P (2010) Theoretical study of Li, Si and Sn adsorption on single-walled boron nitride nanotubes. *J Phys Chem C* 114(13): 5792-5797.
48. Monajjemi M, Lee VS, Khaleghian M, Honarparvar B, Mollaamin F (2010) Theoretical description of electromagnetic nonbonded interactions of radical, cationic, and anionic $\text{NH}_2\text{BHNBNH}_2$ inside of the $\text{B}_{18}\text{N}_{18}$ nanoring. *J Phys Chem C* 114(36): 15315-15330.
49. Monajjemi M (2017) Liquid-phase exfoliation (LPE) of graphite towards graphene: An ab initio study. *Journal of Molecular Liquids* 230: 461-472.
50. Monajjemi M (2012) Quantum investigation of non-bonded interaction between the $\text{B}_{15}\text{N}_{15}$ ring and BH_2NBH_2 (radical, cation, anion) systems: a nanomolecular motor. *Structural Chemistry* 23(2): 551-580.
51. Monajjemi M, Boggs JE (2013) A new generation of B_nN_n rings as a supplement to boron nitride tubes and cages. *J Phys Chem A* 117(7): 1670-1684.
52. Monajjemi M, Khaleghian M (2011) EPR Study of electronic structure of $[\text{CoF}_6]^{3-}$ and $\text{B}_{18}\text{N}_{18}$ nano ring field effects on octahedral complex. *Journal of Cluster Science* 22(4): 673-692.
53. Monajjemi M, Wayne R, Boggs JE (2014) NMR contour maps as a new parameter of carboxyl's OH groups in amino acids recognition: A reason of tRNA-amino acid conjugation. *Chemical Physics* 433: 1-11.
54. Monajjemi M, Falahati M, Mollaamin F (2013) Computational investigation on alcohol nanosensors in combination with carbon nanotube: a Monte Carlo and ab initio simulation. *Ionics* 19(1): 155-164.
55. Monajjemi M, Mollaamin F (2012) Molecular modeling study of drug-DNA combined to single walled carbon nanotube. *Journal of Cluster Science* 23(2): 259-272.

56. Mollaamin F, Monajjemi M (2012) DFT outlook of solvent effect on function of nano bioorganic drugs. *Physics and Chemistry of Liquids* 50(5): 596-604.
57. Monajjemi M, Khosravi M, Honarparvar B, Mollaamin F (2011) Substituent and solvent effects on the structural bioactivity and anticancer characteristic of catechin as a bioactive constituent of green tea. *International Journal of Quantum Chemistry* 111(12): 2771-2777.
58. Monajjemi M (2015) Non-covalent attraction of $B_2N^{(-0)}$ and repulsion of $B_2N^{(+)}$ in the B_nN_n ring: A quantum rotatory due to an external field. *Theoretical Chemistry Accounts* 134:77.
59. Monajjemi M (2014) Metal-doped graphene layers composed with boron nitride-graphene as an insulator: A nano-capacitor *Journal of Molecular Modeling* 20: 2507.
60. Monajjemi M, Khaleghian M, Mollaamin F (2010) Theoretical study of the intermolecular potential energy and second virial coefficient in the mixtures of CH_4 and Kr gases: a comparison with experimental data. *Molecular Simulation* 36(11): 865-870.
61. Monajjemi M (2015) Cell membrane causes the lipid bilayers to behave as variable capacitors: A resonance with self-induction of helical proteins. *Biophysical Chemistry* 207: 114-127.
62. Jalilian H, Monajjemi M (2015) Capacitor simulation including of X-doped graphene (X=Li, Be, B) as two electrodes and $(h-BN)_m$ ($m=1-4$) as the insulator. *Japanese Journal of Applied Physics* 54(8): 085101.
63. Shin S, Jang J (2007) Thiol containing polymer encapsulated magnetic nanoparticles as reusable and efficiently separable adsorbent for heavy metal ions. *Chem Commun* 41: 4230-4232.
64. Oliveira LCA, Petkowicz DI, Smaniotta A, Pergher SBC (2004) Magnetic zeolites: a new adsorbent for removal of metallic contaminants from water. *Water Res* 38(17): 3699-3704.
65. Hu J, Chen G, Lo IMC (2005) Removal and recovery of Cr (VI) from wastewater by maghemite nanoparticles. *Water Res* 39(18): 4528-4536.
66. Yavuz CT, Mayo JT, Yu WW, Prakash A, Falkner JC, et al. (2006) Low-field magnetic separation of monodisperse Fe_3O_4 nanocrystals. *Science* 314(5801): 964-967.
67. Hai B, Wu J, Chen X, Protasiewicz JD, Scherson DA (2005) Metal-Ion adsorption on carboxyl-bearing self-assembled monolayers covalently bound to magnetic nanoparticles. *Langmuir* 21(7): 3104-3105.
68. Hu J, Lo MC, Chen GH (2007) Performance and mechanism of chromate (VI) adsorption by δ -FeOOH-coated maghemite (γ - Fe_2O_3) nanoparticles. *Sep Purif Technol* 58(1): 76-82.
69. Chang YC, Chen DH (2005) Preparation and adsorption properties of monodisperse chitosan-bound Fe_3O_4 magnetic nanoparticles for removal of Cu(II) ions. *J Colloid Interface Sci* 283(2): 446-451.
70. Liu JF, Zhao ZS, Jiang GB (2008) Coating Fe_3O_4 magnetic nano-particles with humic acid for high efficient removal of heavy metals in water. *Environ Sci Technol* 42(18): 6949-6954.
71. Yantasee W, Warner CL, Sangvanich T, Addleman RS, Carter TG, et al. (2007) Removal of heavy metals from aqueous systems with thiol functionalized superparamagnetic nano-particles. *Environ Sci Technol* 41(14): 5114-5119.
72. Kumar M, Rathore DPS, Singh AK (2000) Amberlite XAD-2 functionalized with o-aminophenol: synthesis and applications as extractant for copper(II), cobalt(II), cadmium(II), nickel(II), zinc(II) and lead(II). *Talanta* 51(6):1187-1196.
73. Lam KF, Yeung KL, McKay G (2007) Efficient approach for Cd^{2+} and Ni^{2+} removal and recovery using mesoporous adsorbent with tunable selectivity. *Environ Sci Technol* 41(9): 3329-3334.
74. Li J, Miao X, Hao Y, Zhao J, Sun X, et al. (2008) Synthesis, amino-functionalization of mesoporous silica and its adsorption of Cr(VI). *J Colloid Interface Sci* 318(2): 309-314.
75. Liu Q, Xu Z, Finch JA, Egerton R (1998) A novel two-step silica-coating process for engineering magnetic nano-composites. *Chem Mater* 10(12): 3936-3940.
76. Lu CW, Hung Y, Hsiao JK, Yao M, Chung TH, et al. (2007) Bifunctional magnetic silica nanoparticles for highly efficient human stem cell labeling. *Nano Lett* 7(1): 149-154.
77. Ashtari P, He XX, Wang K, Gong P (2005) An efficient method for recovery of target DNA based on amino-modified silica-coated magnetic nanoparticles. *Talanta* 67(3):548-554.
78. Zhao Y, Truhlar DG (2008) The Mo6 suite of density functionals for main group thermochemistry, thermochemical kinetics, noncovalent interactions, excited states, and transition elements: two new functionals and systematic testing of four Mo6-class functionals and 12 others functional. *Theor Chem Account* 120(1-3):215-241.
79. Zhao, Y, Truhlar, DG (2008) Density functionals with broad applicability in chemistry. *Accounts of Chemical Research* 41(2): 157-167.
80. Grimme S (2006) Seemingly simple stereo electronic effects in alkane isomers and the implications for kohn-sham density functional theory. *ChemInt Ed* (45): 4460-4464.
81. Schreiner PR, Fokin AA, Pascal RA, de Meijere A (2006) Many density functional theory approaches fail to give reliable large hydrocarbon isomer energy differences. *Org Lett* 8(17): 3635-3638.
82. Kohn W, Sham LJ (1965) Self-consistent equations including exchange and correlation effects. *Phys Rev* (140)A: 1133-1138.
83. Perdew JP, Burke K (1996) Generalized gradient approximation made simple. *Phys Rev Lett* (77): 3865-3868.
84. Besler BH, Merz KM, Kollman PA (1990) Atomic charges derived from semiempirical methods. *J comp Chem* 11(4): 431-439.
85. Brneman CM, Wiberg KB (1990) Determining atom-centered monopoles from molecular electrostatic potentials: The need for high sampling density in formamide conformational analysis. *J Comp Chem* 11(3): 361-373.
86. Chirlian LE, Francl MM (1987) Atomic charges derived from electrostatic potentials: A detailed study. *J Comp Chem* 8(6): 894-905.
87. Martin F, Zipse H (2005) Charge distribution in the water molecule-A comparison of methods. *J Comp Chem* 26(1): 97-105.
88. Balderchi A, Baroni S, Resta R (1998) Evolution of the dendritic instability in solidifying succinonitrile. *Phys Rev Lett* (61): 173.
89. Lu T, Chen F (2011) Calculation of molecular orbital composition. *Acta Chim Sinica* 69: 2393-2406.
90. Lu T, Chen F (2012) Quantitative analysis of molecular surface based on improved marching tetrahedral algorithm. *J Mol Graph Model* 38: 314-323.
91. Lu T, Chen F (2012) Multiwfn: A multifunctional wave function analyzer. *J Comp Chem* 33(5): 580-592.



Creative Commons Attribution 4.0
International License

For possible submissions Click Here

Submit Article



Research & Development in Material Science

Benefits of Publishing with us

- High-level peer review and editorial services
- Freely accessible online immediately upon publication
- Authors retain the copyright to their work
- Licensing it under a Creative Commons license
- Visibility through different online platforms